bioengineering

MDPI

Article

Development of Antibacterial Dentures Using Titanium Apatite Peening

Hideaki Sato [1], Akiko Miyake [2], Nichika Harakawa [3], Issei Shoji [1], Yutaka Kameyama [1], Shuhei Kodama [1], Yuichiro Tashiro [4], Chizuko Ogata [5] and Satoshi Komasa [5,*]

[1] Department of Mechanical Engineering, Faculty of Science and Engineering, Tokyo City University, 1-28-1 Tamadutsumi, Setagaya-ku, Tokyo 158-8557, Japan; shsato@tcu.ac.jp (H.S.); tumemiya37@gmail.com (I.S.); ykameya@tcu.ac.jp (Y.K.); skodama@tcu.ac.jp (S.K.)
[2] Department of Oral Health Sciences, Faculty of Health Sciences, Osaka Dental University, 1-4-4, Makino-honmachi, Hirakata-shi 537-1144, Japan; miyake-a@cc.osaka-dent.ac.jp
[3] Mechanics, Graduate School of Integrative Science and Engineering, Tokyo City University, 1-28-1 Tamadutsumi, Setagaya-ku, Tokyo 158-8557, Japan; haranichi0313@gmail.com
[4] Department of Removable Prosthodontics and Occlusion, Osaka Dental University, 8-1 Kuzuha-hanazono-cho, Hirakata-shi 573-1121, Japan; tashiro@cc.osaka-dent.ac.jp
[5] Department of Oral Health Engineering, Faculty of Health Sciences, Osaka Dental University, 1-4-4, Makino-honmachi, Hirakata-shi 537-1144, Japan; ogata-c@cc.osaka-dent.ac.jp
* Correspondence: komasa-s@cc.osaka-dent.ac.jp; Tel.: +81-72-864-3084; Fax: +81-72-864-3184

Abstract

This study investigated antibacterial dentures fabricated by peening titanium apatite onto a polymethyl methacrylate (PMMA) denture base resin using a peening device. The effects of different peening mass flow rates and total peening masses on the deposition and antibacterial properties of titanium apatite were investigated. Titanium apatite was peened onto PMMA specimens at mass flow rates of 1, 2, and 5 g/s, with total peening masses of 5, 10, and 15 g. The surface morphology, elemental distribution, and mass changes were analyzed before and after peening and after immersion and water rinsing. The antibacterial activity against *Staphylococcus aureus* was evaluated using a crystal violet assay. The results showed that reducing the peening mass flow rate increased the amount of titanium apatite transferred and enhanced the antibacterial properties, with the highest deposition achieved at 1 g/s. Varying the total peening mass did not significantly affect the deposition pattern or antibacterial activity. The arithmetic mean roughness of the denture base remained unchanged after peening, indicating its clinical applicability. In conclusion, peening titanium apatite onto PMMA at a lower mass flow rate enabled stronger bonding and incorporation of antibacterial properties, potentially contributing to the development of novel antibacterial denture base materials.

Keywords: titanium apatite; denture base resin; PMMA; antibacterial dentures; peening; transfer; mass flow rate; surface roughness

Academic Editor: Giovanni Vozzi

Received: 14 December 2025
Revised: 2 February 2026
Accepted: 6 February 2026
Published: 15 February 2026

1. Introduction

In recent years, oral frailty has become a significant concern as a super-aged society emerges. Oral frailty leads to an imbalance in dietary habits and reduced social interaction, creating a vicious cycle that results in decreased physical strength and muscle mass, impaired judgment, and cognitive decline [1–5]. One diagnostic criterion for oral frailty is poor oral hygiene and unclean dentures, making oral cavity and denture care a major challenge [1,6,7]. Poor oral hygiene and unclean dentures increase the number

of pathogenic bacteria in the oral cavity [8–10]. Maintaining oral cleanliness—as well as possible—and suppressing oral bacteria proliferation are crucial in preventing oral frailty. Complete and partial dentures are the most common prosthetics used to improve oral quality of life. However, denture plaque deposits adhering to dentures have reportedly caused denture stomatitis, angular cheilitis, and glossitis [11–13]. Furthermore, in older people—who generally have reduced oral function and systemic resistance—the use of unclean dentures with accumulated debris poses the risk of systemic diseases such as fungal infections of the digestive tract or lungs owing to aspiration or accidental ingestion of the fungal flora in denture plaque [2,14,15]. Continuing to wear dentures with poor oral hygiene promotes the accumulation of denture plaque, raising concerns of further oral environment deterioration in the future. Therefore, maintaining oral cleanliness is essential for preserving the quality of life of older people.

Our research team is working to elucidate the detailed mechanisms of stain adhesion and detachment on the denture base surface [16–18]. Miyake et al. revealed that acrylic resin—the primary material used for denture bases—is more prone to staining than dental metal materials, not only because of their surface properties but also from the perspectives of chemical composition and potential difference [16]. Therefore, maintaining oral hygiene in elderly patients is difficult unless improvements are made to both cleaning methods and denture base materials [12,19]. In recent years, the development of novel denture materials based on antimicrobial substance coatings applied to the denture surface has been advanced as an approach to establish simpler and safer denture cleaning methods for denture wearers [2,19,20].

This material, termed a self-cleaning denture, is expected to become a self-cleaning denture base material and has been reported in various studies [21–25]. However, increasing the concentration of this material may reduce the mechanical properties of the denture base material. For dentures to function effectively in the oral cavity, the denture material must possess sufficient strength to withstand chewing forces. Fujitsu, in collaboration with the Research Center for Advanced Science and Technology at the University of Tokyo, has developed a novel photocatalyst, calcium hydroxide hydroxyapatite (TiHA), with excellent adsorption properties. Direct incorporation of this material into resin reportedly causes minimal degradation of the resin relining material, making it a promising approach for applications in electronic devices and sanitary products. In this study, we investigated whether incorporating TiHA into polymethyl methacrylate (PMMA) could yield an antibacterial denture base material.

Our previous study demonstrated that incorporating TiHA into denture base materials imparts antibacterial properties against *Staphylococcus aureus* and inhibits the adhesion of salivary proteins involved in bacterial adhesion, without compromising mechanical strength [17]. Furthermore, in vitro evaluations using epithelial cells demonstrated no cytotoxicity, suggesting its potential as a clinically applicable material. However, concerns remained regarding the lack of established long-term antimicrobial efficacy and potential degradation of antimicrobial properties resulting from the deterioration of the denture base material. Therefore, titanium apatite must be uniformly distributed on the denture base surface to maintain long-term antimicrobial properties.

This study aimed to develop a denture base surface treatment method that firmly deposits titanium apatite onto denture base materials via peening, thereby imparting antibacterial properties without compromising mechanical properties.

2. Materials and Methods

2.1. Effect of Peening Mass Flow Rate on Titanium Apatite Transfer

2.1.1. Peening Apparatus

Figure 1 shows a schematic of the peening apparatus. Using a compressor, air is compressed and stored in a tank. A pressure-reducing valve is connected to this tank to regulate the air to a constant pressure. Pressure-regulated air is fed through the nozzle to perform peening. A shot-peening nozzle was used in this study.

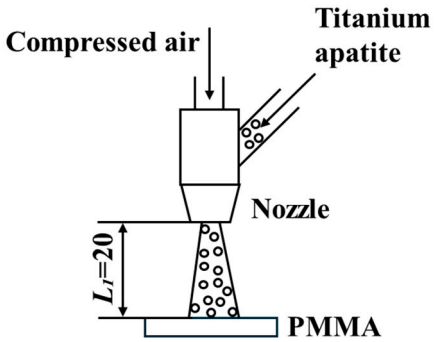

Figure 1. Peening apparatus.

2.1.2. Particles and Test Specimens

For this study, we prepared TiHA powder (PHOTOHAP PCAP-100, Taihei Chemical Industrial Co., Ltd., Osaka, Japan). Figure 2 shows the morphology of the TiHA particles, measured using a Morphologi 4 (Malvern Panalytical, Tokyo, Japan). The circle evaluated diameter was determined to be 1.94 μm. The chemical formula of normal HA is $Ca_{10}(OH)_2(PO_4)_6$. However, in TiHA, some Ca^{2+} is replaced by Ti^{4+}. The TiHA had a specific surface area of 30–70 m^2/g. Experimental denture base resin test specimens were prepared using a polymer powder of PMMA-based self-curing denture base resin (ACRON MC, dupe pink, GC Co., Tokyo, Japan). Using waterproof abrasive paper (Riken Corundum, Ltd., Konosu, Japan) in the order of #800, #1000, and #1500, all test specimens were polished into cylindrical disk (diameters = 15 mm, thickness = 1 mm) or bar-shaped (diameters = 9 mm, thicknesses = 10 mm) test specimens. Ultrasonic cleaning was performed after polishing, after which the samples were stored in water. The disk-shaped test specimens were used for surface observation and antibacterial activity evaluation.

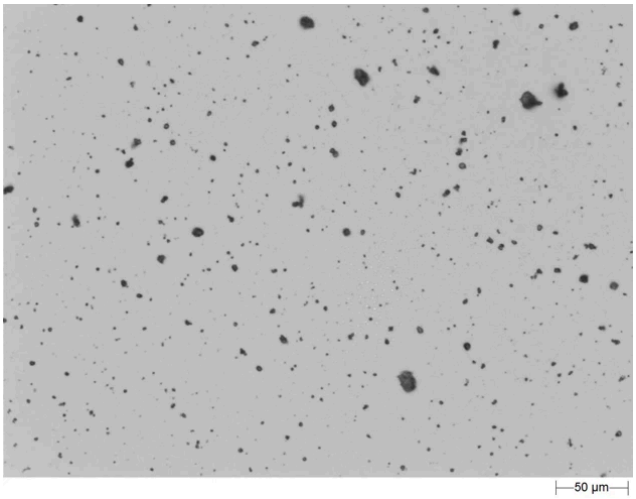

Figure 2. Titanium hydroxyapatite (Automated particle image analysis) (automated particle image analysis).

2.1.3. Experimental Conditions and Evaluation Methods

The surface roughness of the denture base resin (PMMA) specimens was polished by wet polishing with silicon carbide abrasive waterproof abrasive paper having grain sizes ranging from #600 to #1200, thereby achieving an arithmetic mean roughness *Ra* of $0.14 \leq Ra \leq 0.20$ µm. Subsequently, titanium apatite was sprayed onto the PMMA specimens at a perpendicular projection angle using the aforementioned peening apparatus under the peening conditions listed in Table 1.

Table 1. Peening conditions.

Pressure P MPa	0.6
Peening distance L_1 mm	20
Total peening mass m g	10
Peening mass flow rate g/s	1, 2, 5
Number of peening n times	1

The specimens were then immersed in 100 mL of distilled water at approximately 36 °C for 10 d. Subsequently, tap water was flowed perpendicular to the transfer surface of the specimens under the water flow conditions listed in Table 2. The masses of the specimens after water flow were measured to determine the mass changes before and after peening. The surface morphologies and elemental distributions of the specimens were observed using scanning electron microscopy (Miniscope TM3000; Hitachi High-Tech Corporation, Tokyo, Japan). In addition, the area ratio of the region where the particles had transferred to were calculated using ImageJ (NIH, Bethesda, MD, USA, https://imagej.nih.gov/ij/, accessed on 1 February 2026).

Table 2. Water flow conditions.

Distance Between the Tap and the Test Specimen L_2 mm	200
Angle θ°	90
Flow rate Q m^3/s	3.0×10^{-5}
Water flow time min	40

2.1.4. Antimicrobial Evaluation

Staphylococcus aureus (ATCC 12600; American Type Culture Collection, Manassas, VA, USA) was cultured in tryptic soy broth (TSB) and tryptic soy agar (TSA). A single colony was selected and cultured overnight in 10 mL of TSB at 37 °C. The cells were then diluted in fresh TSB to approximately 1×10^9 CFU/mL. To evaluate biofilm formation, *Staphylococcus aureus* seed cultures were prepared and diluted to optical densities of 0.1 and 1.0. These cultures were plated onto disks and incubated for 6–24 h. To evaluate biofilm formation, the disks were washed with PBS, incubated at room temperature for 20 min with 2 mL of 0.05% *w*/*v* crystal violet dye, washed three times with PBS to remove residual dye, transferred to a new 12-well plate, and decolorized by rotating and agitating at room temperature for 20 min in 1 mL of 95% ethanol. After decolorization, 100 µL of ethanol was added to each well, and the absorbance at 595 nm was measured using a SpectraMax M5 (Molecular Devices, CA, USA) 96-well microplate reader.

2.2. Effect of Total Peening Mass on Titanium Apatite Transfer

2.2.1. Experimental Conditions and Evaluation Methods

The surface roughness of denture base resin (PMMA) specimens was polished by wet polishing with silicon carbide abrasive waterproof abrasive paper having grain sizes from #600 to #1200, thereby achieving an arithmetic mean roughness *Ra* within the range of $0.14 \leq Ra \leq 0.20$ µm. Subsequently, titanium apatite was peened onto the PMMA specimens at a perpendicular projection angle using the aforementioned peening apparatus under the conditions listed in Table 3. The test specimens were then immersed in 100 mL of distilled water at approximately 36 °C for 10 d. Subsequently, tap water was flowed perpendicular to the transfer surface of the test specimens under the water flow conditions listed in Table 2. The masses of the test specimens after water flow were measured to determine the mass change between the pre- and post-peening states. In addition, surface morphologies and element distributions of the test specimens were observed using scanning electron microscopy (Miniscope TM3000, Hitachi High-Tech Corporation, Tokyo, Japan). Finally, using ImageJ, the area ratio of the region where particles had transferred to were calculated.

Table 3. Peening conditions.

Pressure *P* MPa	0.6
Peening distance L_1 mm	20
Total peening mass *m* g	5, 10, 15
Peening mass flow rate g/s	1
Number of peening *n* times	1

2.2.2. Antimicrobial Evaluation

Staphylococcus aureus (ATCC 12600; American Type Culture Collection, Manassas, VA, USA) was cultured in TSB and TSA. A single colony was selected and cultured overnight in 10 mL of TSB at 37 °C. The cells were then diluted in fresh TSB to approximately 1×10^9 CFU/mL. To evaluate biofilm formation, S. aureus seed cultures were prepared and diluted to optical densities of 0.1 and 1.0. These cultures were plated onto disks and incubated for 6–24 h. To evaluate biofilm formation, the disks were washed with PBS, incubated at room temperature for 20 min with 2 mL of 0.05% *w*/*v* crystal violet dye, washed three times with PBS to remove residual dye, transferred to a new 12-well plate, and decolorized by rotating and agitating at room temperature for 20 min in 1 mL of 95% ethanol. After decolorization, 100 µL of ethanol was added to each well, and the absorbance at 595 nm was measured using a SpectraMax M5 96-well microplate reader.

2.3. Statistical Analysis

Each measurement was performed three times, and statistical analyses were performed using one-way analysis of variance. The Mann–Whitney U Test was used to determine significant differences. The significance level was set at <5%.

3. Results

3.1. Effect of Peening Mass Flow Rate on Titanium Apatite Transfer

3.1.1. Surface and Mass Analysis After Water Flow Testing

Figure 3A,B show optical microscopy images of the peened surface at different peening mass flow rates as well as those of the peened specimen surfaces after immersion and water flow. After peening, the specimen with a peening mass flow rate of 5 g/s exhibits the highest titanium apatite transfer. However, after immersion and water flow, the particles

peeled off. For peening mass flow rates of 1 and 2 g/s, little difference can be observed in the transfer pattern.

(**A**)

Pressure P MPa	0.6	0.6	0.6
Peening distance L_1 mm	20	20	20
Total peening mass m g	10	10	10
Peening mass flow rate g/s	1	2	5
After peening (×20)	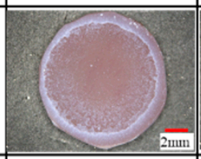	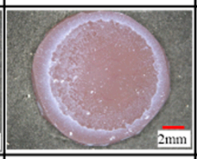	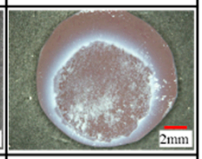
After immerse (×20)	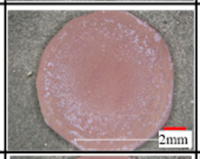	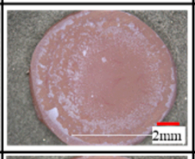	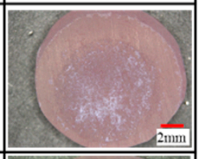
After water flow (×20)	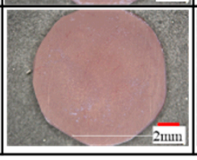	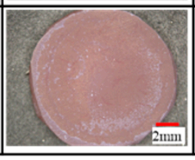	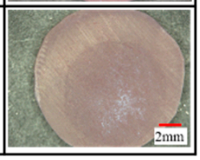

(**B**)

Pressure P MPa	0.6	0.6	0.6
Peening distance L_1 mm	20	20	20
Total peening mass m g	10	10	10
Peening mass flow rate g/s	1	2	5
After peening (×200)	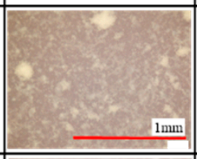	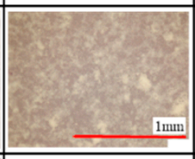	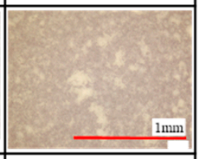
After immerse (×200)	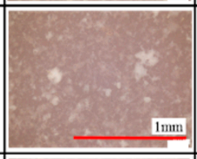	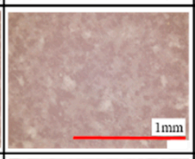	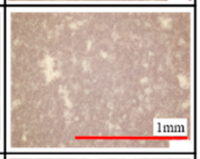
After water flow (×200)	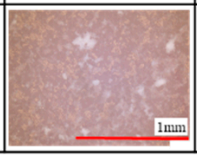	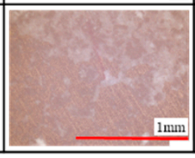	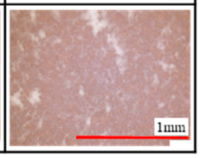

Figure 3. Optical microscopy images. (**A**) 20× magnification image (**B**) 200× magnification image.

Figure 4 shows the surface analysis images before peening and after water flow. The surface analysis image after water flow reveals the presence of P, Ca, and Ti, confirming the transfer of titanium apatite onto the test specimen.

Figure 5 shows a binary image of the test specimen after water flow, processed in ImageJ. Figure 6 shows the area ratio of the transferred portion calculated from a binarized image. No significant difference can be observed between the peening mass flow rates of 1, 2, and 5 g/s. However, because this area fraction measurement reflects only the surface condition, it is conceivable that reducing the peening mass flow rate increases the particle transfer intensity, despite no significant observable difference.

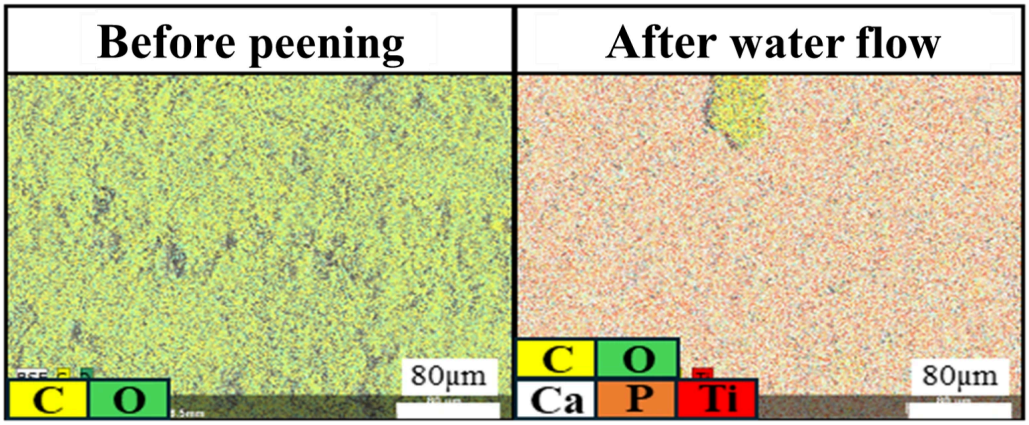

Figure 4. Surface analysis images before peening and after water flow.

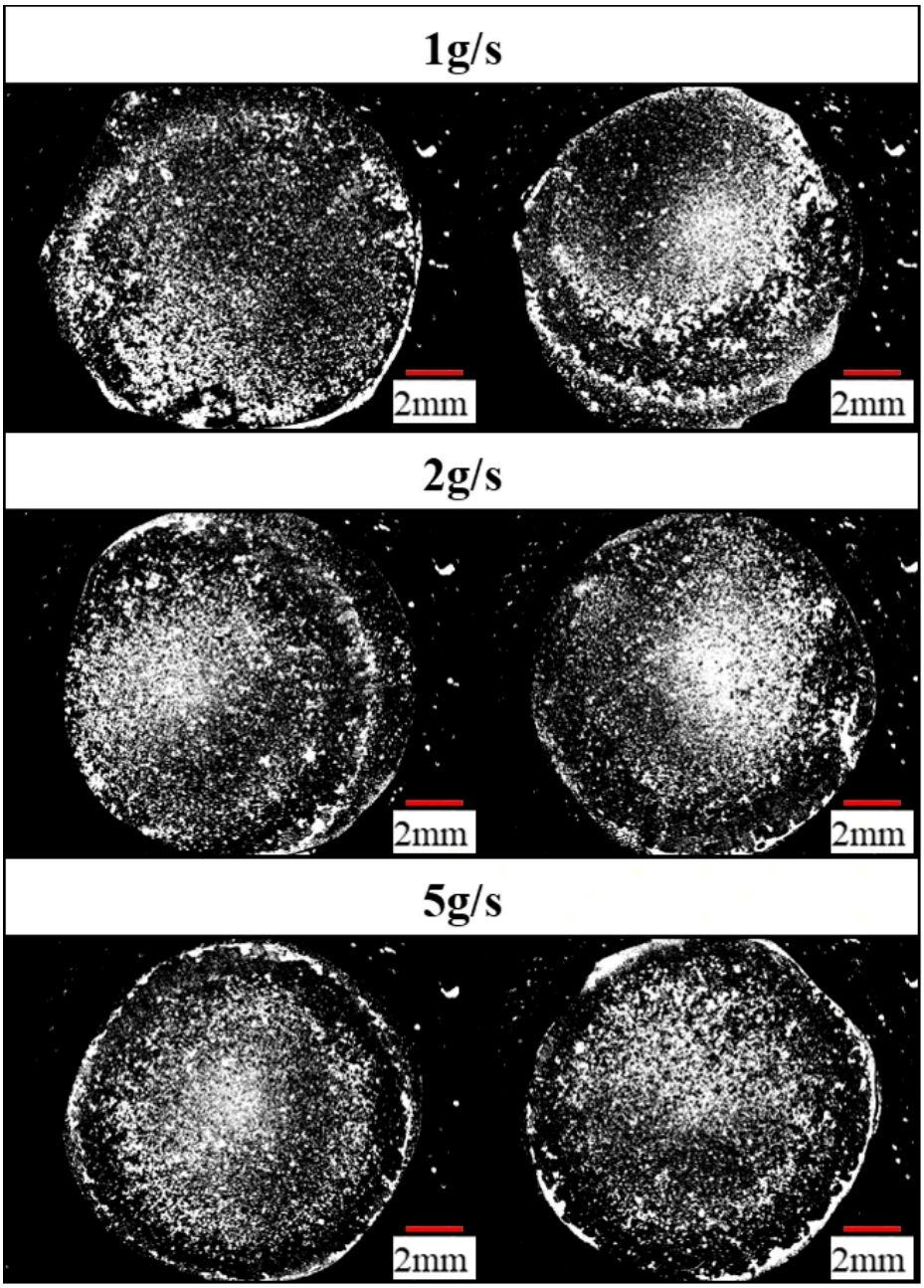

Figure 5. Binary image of the test specimen after water flow, processed in ImageJ.

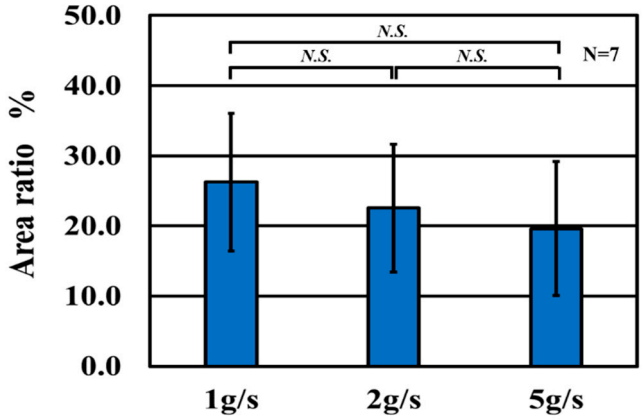

Figure 6. Area ratio of the transferred portion calculated from a binarized image.

Figure 7 shows the mass increase before and after peening and after water flow. After peening, the 5 g/s condition exhibits the highest titanium apatite transfer. However, the mass decreases significantly after immersion and water flow, reaching the lowest value measured.

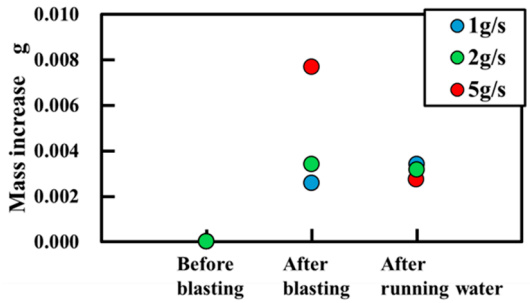

Figure 7. Mass increase before and after peening and after water flow.

Figure 8 shows a comparison of the arithmetic mean surface roughness *Ra* before peening and that after ultrasonic cleaning following water flow. Regardless of the peening conditions, no significant difference can be observed between the pre-peening and post-ultrasonic cleaning conditions.

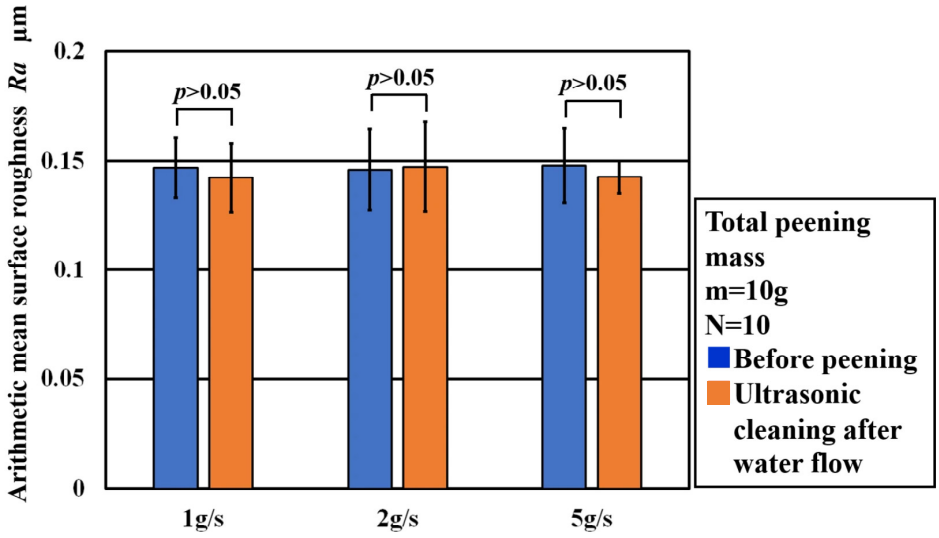

Figure 8. Comparison of the arithmetic mean surface roughness *Ra* before peening and that after ultrasonic cleaning following water flow.

3.1.2. Antimicrobial Evaluation

Figure 9 shows the relationship between the peening mass flow rate and absorbance. As absorbance decreases, antibacterial activity is recognized; as absorbance increases, antibacterial activity is not recognized. Significant differences can be observed between the no peening condition and the titanium apatite peening mass flow rates of 1, 2, and 5 g/s. Furthermore, although no significant difference can be observed between 1 and 2 g/s, significant differences are found between 1 and 5 g/s and between 2 and 5 g/s.

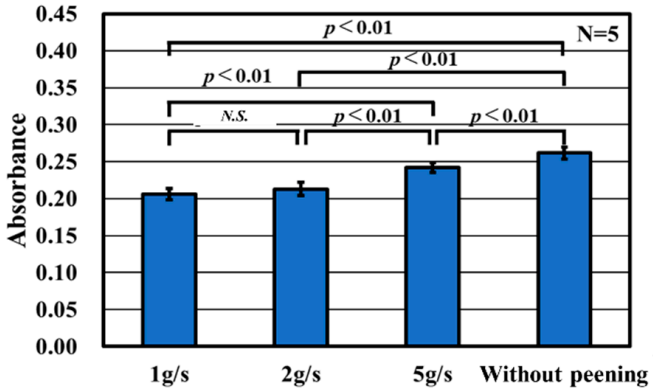

Figure 9. Relationship between the peening mass flow rate and absorbance.

Figure 10 shows the relationship between the absorbance and area ratio of the transferred region. As the area ratio of the transferred region increases, the absorbance decreases almost in proportion.

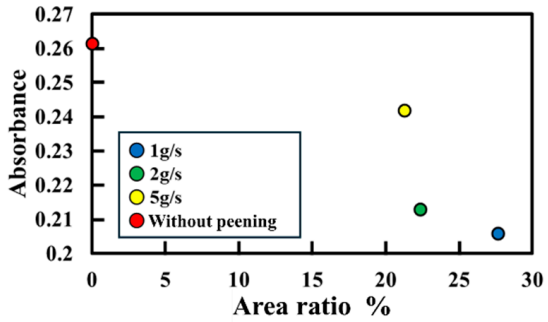

Figure 10. Relationship between the absorbance and area ratio of the transferred region.

Figure 11 shows the relationship between absorbance and mass increase after water flow. As mass increased due to transfer, absorbance decreased.

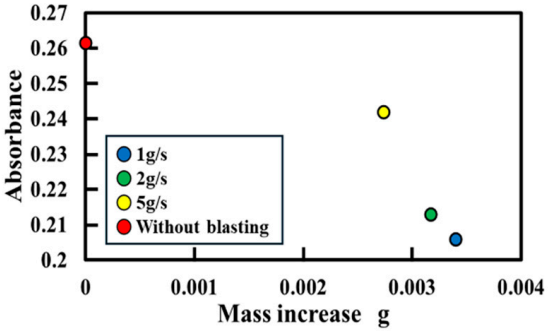

Figure 11. Relationship between absorbance and mass increase after water flow.

3.2. Effect of Total Peening Mass on Titanium Apatite Transfer

3.2.1. Experimental Conditions and Evaluation Methods

Figure 12A,B show optical microscopy images of the peened surface at different total peening mass as well as those of the peened specimen surfaces after immersion and water flow. Titanium apatite transferred to the surface, regardless of the total peening mass. However, no differences in transfer patterns are observable.

(A)

Pressure P MPa	0.6	0.6	0.6
Peening distance L_1 mm	20	20	20
Total peening mass m g	5	10	15
Peening mass flow rate g/s	1	1	1
After peening (×20)			
After immerse (×20)	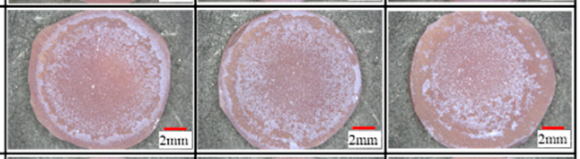		
After water flow (×20)	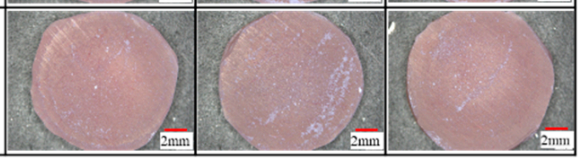		

(B)

Pressure P MPa	0.6	0.6	0.6
Peening distance L_1 mm	20	20	20
Total peening mass m g	5	10	15
Peening mass flow rate g/s	1	1	1
After peening (×200)	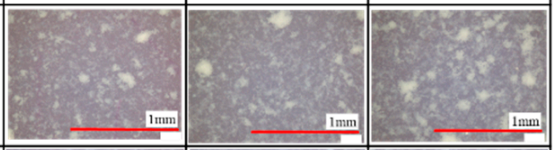		
After immerse (×200)	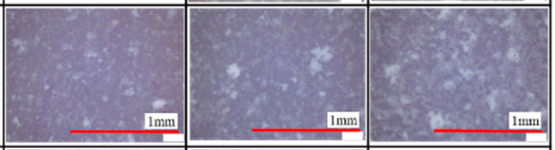		
After water flow (×200)	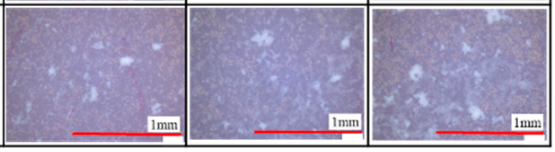		

Figure 12. Optical microscopy images. (**A**) 20× magnification image (**B**) 200× magnification image.

Figure 13 shows a binary image of the test specimen after water flow, processed in Image J.

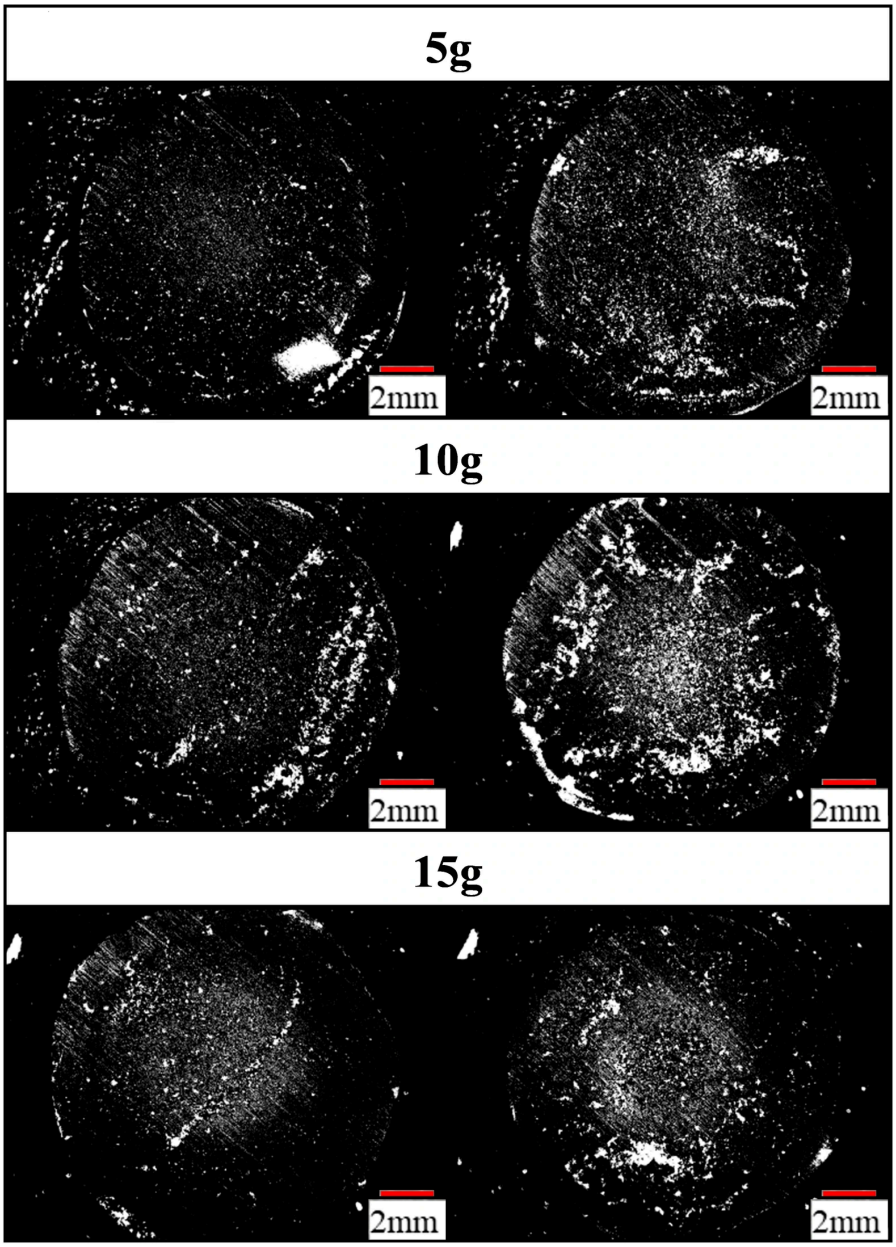

Figure 13. Binary image of the test specimen after water flow, processed in ImageJ.

Figure 14 shows the area ratio of the transferred portion calculated from a binarized image. Among the three total peening masses (5, 10, and 15 g), 10 g exhibits the greatest area ratio of transferred material.

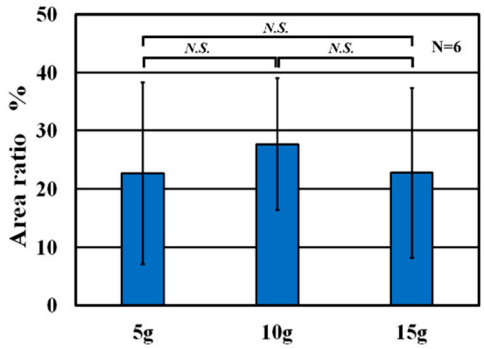

Figure 14. Area ratio of the transferred portion calculated from a binarized image.

Figure 15 shows the increase in mass before peening, after peening, and after water flow. After peening and water flow, the 15 g total peening mass condition exhibits the largest increase in mass.

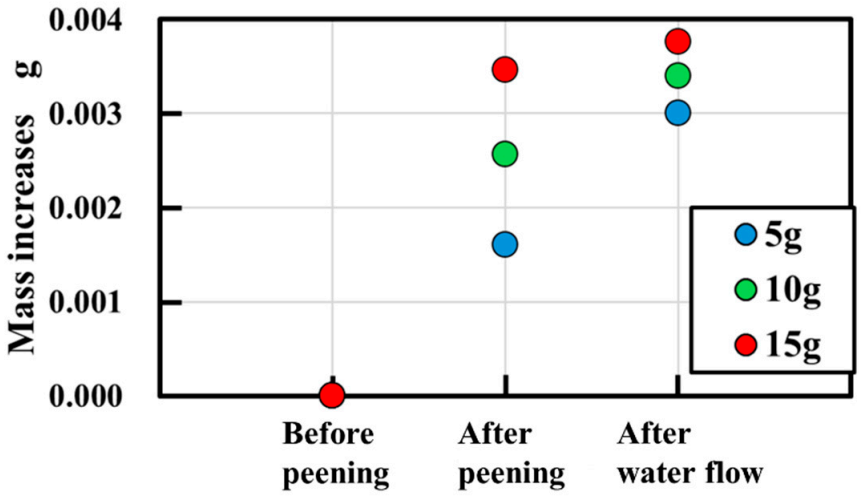

Figure 15. Increase in mass before peening, after peening, and after water flow.

Figure 16 shows a comparison of the arithmetic mean surface roughness *Ra* before peening and that after ultrasonic cleaning following water flow. Regardless of the peening conditions, little change in the arithmetic mean surface roughness *Ra* can be observed between ultrasonic cleaning without peening and ultrasonic cleaning after water flow.

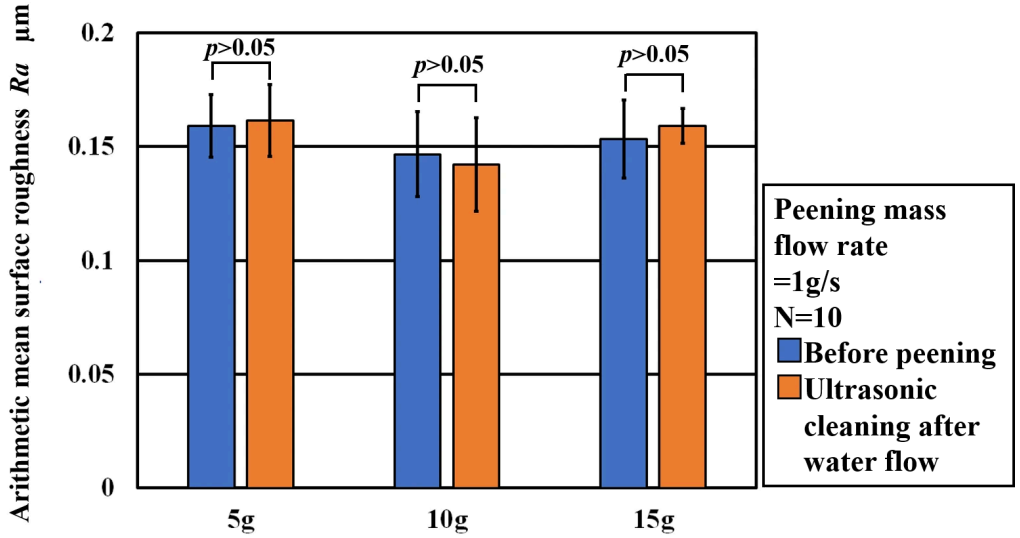

Figure 16. Comparison of the arithmetic mean surface roughness *Ra* before peening and that after ultrasonic cleaning following water flow.

3.2.2. Antimicrobial Evaluation

Figure 17 shows the relationship between the total peening mass and absorbance. A decrease in absorbance indicates antibacterial activity. Absorbance can be observed to be the highest when no peening is applied. As the total peening mass decreases, absorbance also decreases.

Figure 18 shows the relationship between absorbance and mass increase. When peening is applied, the absorbance increases as the mass increase became larger.

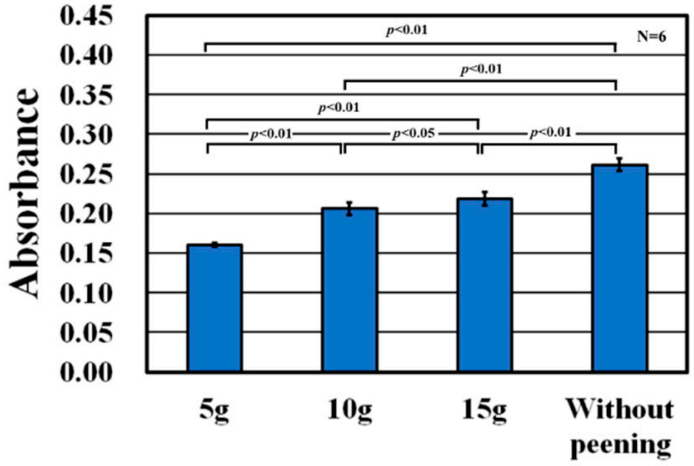

Figure 17. Relationship between the total peening mass and absorbance.

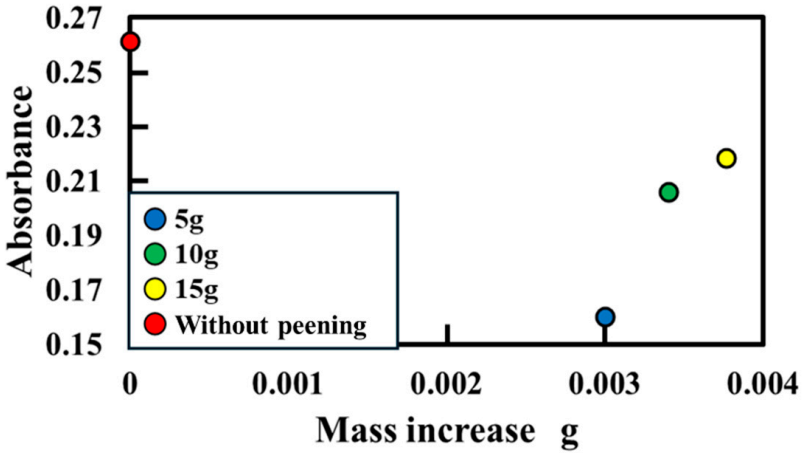

Figure 18. Relationship between absorbance and mass increase after water flow.

Figure 19 shows the relationship between absorbance and area ratio. No correlation between the total peening mass and the area ratio is observable, nor one between the absorbance and area ratio.

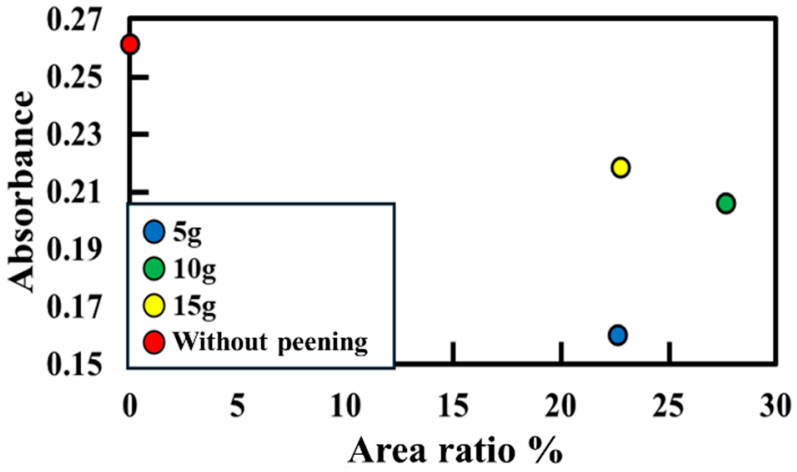

Figure 19. Relationship between absorbance and area ratio after water flow.

4. Discussion

PMMA—the primary component of the dentures used in this experiment—possesses high strength and transparency, with a glass transition temperature of 110 °C [26–28]. The

resin base discolors with long-term use because of stains and plaque adhering to its surface, necessitating regular cleaning. Acrylic resin is not capable of maintaining mechanical or chemical cleanliness, nor can it sustain long-term mechanical properties [5,29,30]. To maintain the cleanliness of these dentures, methods to impart or maintain antimicrobial properties on the dentures must be explored. Therefore, we verified whether TiHA particles could be transferred onto the surface of PMMA using a spray device developed at Tokyo City University.

TiHA ($Ca_{10}(PO_4)_6(OH)_2$) used in this experiment is a novel photocatalyst material in which a part of the Ca in HA is substituted with Ti [31–35]. HA is an adsorbent and does not require an adsorbent layer such as titanium dioxide [36,37]. We investigated the effects of biofilms formed on denture base resins. We demonstrated that TiHA incorporated into denture base resins exhibits antibacterial activity against multiple bacteria, not just a single strain. The antibacterial activity of HA is thought to be attributed to Ca^{2+}, alkaline-earth metal ions, or hydroxyl ions, which have been reported to act as active membrane bactericides that stabilize and kill *Staphylococcus aureus* in the stationary phase [38–40]. Although hydroxyl ions are highly reactive oxidizing agents with lethal effects on bacterial cells, the antibacterial activity of Ca and hydroxyl ions is limited. However, incorporating titanium into HA enhances its photocatalytic properties by generating reactive oxygen species under light irradiation, thereby enhancing antibacterial effects. This photocatalytic activity disrupts bacterial cell membranes and inhibits biofilm formation on denture base resin. Consequently, TiHA offers a promising approach for preventing denture-related infections through sustained antibacterial activity. However, our previous studies have shown that antibacterial activity is observed even in the absence of photocatalytic activity, suggesting their potential for clinical application.

In this study, we first investigated the effect of changing the peening mass flow rate of TiHA peening on the antibacterial properties of the denture material surface. After peening, the 5 g/s sample exhibited the highest titanium apatite transfer. However, after immersion and water flow, the mass decreased significantly, and the increase in mass after water flow was minimal. These results indicate that increasing the peening mass flow rate results in a significant increase in mass immediately after peening; however, the adhesion strength was low, and particles detached upon water flow. Furthermore, although the pattern of mass increase was nearly identical for 1 and 2 g/s, the mass increase after water flow was most significant at 1 g/s. Therefore, the highest titanium apatite transfer was achieved at a peening mass flow rate of 1 g/s. This indicates that, for a constant total peening mass, reducing the peening mass flow rate increases the amount of titanium apatite transferred, demonstrating its antibacterial properties. The results can be attributed to the high peening mass flow rates and increased particle collisions and agglomeration conditions in which particles are easily dislodged by immersion or water flow. In contrast, at low peening mass flow rates, particles are dispersed more uniformly, allowing for more even transfer on the surface and potentially stronger adhesion. These results indicate that altering the peening mass flow rate during titanium apatite peening does not change the surface roughness of the denture base, suggesting its clinical applicability. These findings suggest that optimizing the peening mass flow rate is crucial for enhancing the antibacterial efficacy of denture materials. In addition, maintaining a low peening mass flow rate can improve the durability of titanium apatite peening under clinical conditions involving exposure to saliva and cleaning fluids. Future studies should focus on evaluating the long-term stability and antibacterial performance of coatings applied at different peening mass flow rates in simulated oral environments.

Second, we examined the effect of different total peening masses of TiHA on the antibacterial properties of the denture material surface. Although titanium apatite transfer

was confirmed in all specimens with altered total peening mass, no differences in transfer patterns were observed. Furthermore, when peening was performed with a constant peening mass flow rate but varying total peening mass, the specimens exhibited more antibacterial properties than those of the non-peened control. However, the results showed no clear correlation—antibacterial activity peaked at a total peening mass of 5 g, area coverage of the transferred portion was highest at 10 g, and mass increase was at a maximum at 15 g. The results for absorbance and transfer area ratio indicated that the adhesion strength between titanium apatite and the denture base surface remained low even as the total peening mass increased. In other words, even considering the first experiment, rather than varying the total peening mass, transferring titanium apatite onto the denture base surface at a lower peening mass flow rate clearly enabled stronger adhesion and antibacterial properties. This suggests that optimizing the peening mass flow rate is more critical than simply increasing the total peening mass for the effective transfer of titanium apatite. A lower peening mass flow rate likely promotes better adhesion by enabling more controlled particle impact and greater adhesion to the denture base surface. Future studies should systematically evaluate the influence of peening parameters on both adhesion strength and antibacterial efficacy to establish optimal application conditions.

This study has some limitations. These limitations may affect the generalizability of our findings and should be considered when interpreting our results. In addition to those already mentioned, future research should employ larger sample sizes and more diverse populations. Furthermore, incorporating longitudinal designs would help to establish causal relationships more effectively. Finally, in vivo studies confirming biocompatibility would be advantageous to promote clinical application.

5. Conclusions

In this study, titanium apatite was peened and transferred onto PMMA—a resin material for denture bases. Antibacterial properties were observed at peening mass flow rates of 1, 2, and 5 g/s. Test specimens peened with total peening masses of 5, 10, and 15 g exhibited antibacterial properties comparative to those of non-peened specimens; however, no difference in transfer amount was observed. In other words, maintaining a constant total peening mass while reducing the peening mass flow rate increased the transfer amount, thereby improving antibacterial properties. This finding is expected to contribute to the development of novel denture base materials that can transfer titanium apatite and maintain long-term antibacterial properties.

Author Contributions: H.S., S.K. (Shuhei Kodama) and Y.K. conceived and designed the experiments; A.M., N.H., I.S.. and Y.K. performed the experiments; Y.T. and C.O. analyzed the data; S.K. (Satoshi Komasa) and H.S. wrote the paper. All authors have read and agreed to the published version of the manuscript.

Funding: This research was funded by The Japan Society for the Promotion of Science KAKENHI, grant number 24K13017.

Institutional Review Board Statement: Not applicable.

Informed Consent Statement: Not applicable.

Data Availability Statement: No new data were created or analyzed in this study. Data sharing is not applicable to this article.

Acknowledgments: The authors would like to thank Toru Takagi and Akira Aoki of the Tokyo Medical and Dental University.

Conflicts of Interest: The authors declare no conflicts of interest.

References

1. Tuuliainen, E.; Nihtilä, A.; Nykänen, I.; Suominen, A.L.; Komulainen, K.; Tiihonen, M.; Hartikainen, S. The Association of Frailty with Oral Cleaning Habits and Oral Hygiene among Elderly Home Care Clients. *Scand. J. Caring Sci.* **2019**, *34*, 938–947. [CrossRef]
2. Kanlı, A.; Demirel, F.; Sezgin, Y. Oral Candidosis, Denture Cleanliness and Hygiene Habits in an Elderly Population. *Aging Clin. Exp. Res.* **2005**, *17*, 502–507. [CrossRef]
3. Çankaya, Z.T.; Yurdakoş, A.; Kalabay, P.G. The Association between Denture Care and Oral Hygiene Habits, Oral Hygiene Knowledge and Periodontal Status of Geriatric Patients Wearing Removable Partial Dentures. *Eur. Oral Res.* **2020**, *54*, 9–15. [CrossRef] [PubMed]
4. Moussa, A.R.; Dehis, W.M.; Elboraey, A.N.; Elgabry, H.S. A Comparative Clinical Study of the Effect of Denture Cleansing on the Surface Roughness and Hardness of Two Denture Base Materials. *Open Access Maced. J. Med. Sci.* **2016**, *4*, 476–481. [CrossRef]
5. Rocha, M.M.; Carvalho, A.M.; Coimbra, F.C.T.; De Arruda, C.N.F.; Oliveira, V.D.C.; Macedo, A.P.; Silva-Lovato, C.H.; Pagnano, V.O.; Paranhos, H.D.F.O. Complete Denture Hygiene Solutions: Antibiofilm Activity and Effects on Physical and Mechanical Properties of Acrylic Resin. *J. Appl. Oral Sci.* **2021**, *29*, e20200948. [CrossRef]
6. Müller, F. Oral Hygiene Reduces the Mortality from Aspiration Pneumonia in Frail Elders. *J. Dent. Res.* **2014**, *94*, 14S–16S. [CrossRef] [PubMed]
7. Watanabe, Y.; Yamazaki, Y.; Okada, K.; Kondo, M.; Matsushita, T.; Nakazawa, S. Oral Health for Achieving Longevity. *Geriatr. Gerontol. Int.* **2020**, *20*, 526–538. [CrossRef] [PubMed]
8. Ishikawa, A.; Miyake, Y.; Yoneyama, T.; Miyatake, K.; Hirota, K. Professional Oral Health Care Reduces the Number of Oropharyngeal Bacteria. *J. Dent. Res.* **2008**, *87*, 594–598. [CrossRef]
9. Senpuku, H.; Tsuha, Y.; Hanada, N.; Miyazaki, H.; Inoshita, E.; Sogame, A. Systemic Diseases in Association with Microbial Species in Oral Biofilm from Elderly Requiring Care. *Gerontology* **2003**, *49*, 301–309. [CrossRef]
10. Salerno, C.; Esposito, V.; Guida, A.; Milillo, L.; Pascale, M.; Petruzzi, M.; Contaldo, M.; Busciolano, M.; Serpico, R. Candida-Associated Denture Stomatitis. *Med. Oral* **2011**, *16*, e139–e143. [CrossRef]
11. Addy, M.; Bates, J.F. Plaque Accumulation Following the Wearing of Different Types of Removable Partial Dentures. *J. Oral Rehabil.* **1979**, *6*, 111–117. [CrossRef] [PubMed]
12. Baba, Y.; Sato, Y.; Owada, G.; Minakuchi, S. Effectiveness of a Combination Denture-Cleaning Method versus a Mechanical Method: Comparison of Denture Cleanliness, Patient Satisfaction, and Oral Health-Related Quality of Life. *J. Prosthodont. Res.* **2018**, *62*, 353–358. [CrossRef] [PubMed]
13. Iosif, L.; Dimitriu, B.; Țâncu, A.M.C.; Amza, O.E.; Imre, M.; Pantea, M.; Ispas, A. Qualitative Assessment of the Removable Denture Microbiome. *Germs* **2024**, *14*, 28–37. [CrossRef]
14. Hannah, V.E.; O'Donnell, L.; Robertson, D.; Ramage, G. Denture Stomatitis: Causes, Cures and Prevention. *Prim. Dent. J.* **2017**, *6*, 46–51. [CrossRef]
15. Perić, M.; Miličić, B.; Živković, R.; Arsenijević, V.A.; Pfićer, J.K. A Systematic Review of Denture Stomatitis: Predisposing Factors, Clinical Features, Etiology, and Global *Candida* Spp. Distribution. *JoF* **2024**, *10*, 328. [CrossRef] [PubMed]
16. Miyake, A.; Komasa, Y.; Hashimoto, Y.; Okazaki, J.; Komasa, S. Adsorption of Saliva Related Protein on Denture Materials: An X-Ray Photoelectron Spectroscopy and Quartz Crystal Microbalance Study. *Adv. Mater. Sci. Eng.* **2016**, *2016*, 5478326. [CrossRef]
17. Komasa, S.; Tashiro, Y.; Miyake, A.; Matsumoto, T.; Wang, X.; Nakai, M.; Sato, H.; Hashimoto, Y. Development of a New Self-Cleaning Denture Base Material Using Titanium Apatite. *Dent. Mater. J.* **2025**, *44*, 365–374. [CrossRef]
18. Sato, W.; Hasegawa, Y.; Yoshida, Y.; Okazaki, J.; Komasa, S. Antimicrobial Effect of Titanium Hydroxyapatite in Denture Base Resin. *Appl. Sci.* **2018**, *8*, 963. [CrossRef]
19. Kulak-Ozkan, Y.; Arikan, A.; Kazazoglu, E. Oral Hygiene Habits, Denture Cleanliness, Presence of Yeasts and Stomatitis in Elderly People. *J. Oral Rehabil.* **2002**, *29*, 300–304. [CrossRef]
20. Choo, A.; Delac, D.M.; Messer, L.B. Oral Hygiene Measures and Promotion: Review and Considerations. *Aust. Dent. J.* **2001**, *46*, 166–173. [CrossRef]
21. Takahashi, Y.; Hamanaka, I.; Shimizu, H. Effect of Thermal Shock on Mechanical Properties of Injection-Molded Thermoplastic Denture Base Resins. *Acta Odontol. Scand.* **2011**, *70*, 297–302. [CrossRef] [PubMed]
22. Sasaki, H.; Kawaguchi, T.; Hamanaka, I.; Takahashi, Y. Effect of Long-Term Water Immersion or Thermal Shock on Mechanical Properties of High-Impact Acrylic Denture Base Resins. *Dent. Mater. J.* **2016**, *35*, 204–209. [CrossRef]
23. Aldegheishem, A.; Aldeeb, M.; Al-Ahdal, K.; Helmi, M.; Alsagob, E.I. Influence of Reinforcing Agents on the Mechanical Properties of Denture Base Resin: A Systematic Review. *Polymers* **2021**, *13*, 3083. [CrossRef]
24. Polychronakis, N.C.; Polyzois, G.L.; Lagouvardos, P.E.; Papadopoulos, T.D. Effects of Cleansing Methods on 3-D Surface Roughness, Gloss and Color of a Polyamide Denture Base Material. *Acta Odontol. Scand.* **2014**, *73*, 353–363. [CrossRef]
25. Khan, A.A.; Fareed, M.A.; Alshehri, A.H.; Aldegheishem, A.; Alharthi, R.; Saadaldin, S.A.; Zafar, M.S. Mechanical Properties of the Modified Denture Base Materials and Polymerization Methods: A Systematic Review. *IJMS* **2022**, *23*, 5737. [CrossRef] [PubMed]

26. Matsuo, H.; Suenaga, H.; Suzuki, O.; Takahashi, N.; Takahashi, M.; Sasaki, K. Deterioration of Polymethyl Methacrylate Dentures in the Oral Cavity. *Dent. Mater. J.* **2015**, *34*, 234–239. [CrossRef]
27. Vallittu, P.K. A Review of Methods Used to Reinforce Polymethyl Methacrylate Resin. *J. Prosthodont.* **1995**, *4*, 183–187. [CrossRef] [PubMed]
28. Heimer, S.; Stawarczyk, B.; Schmidlin, P.R. Discoloration of PMMA, Composite, and PEEK. *Clin. Oral Investig.* **2016**, *21*, 1191–1200. [CrossRef]
29. Arai, T.; Sugiyama, T.; Ueda, T.; Sakurai, K. Inhibiting Microbial Adhesion to Denture Base Acrylic Resin by Titanium Dioxide Coating. *J. Oral Rehabil.* **2009**, *36*, 902–908. [CrossRef]
30. Bajunaid, S.O. How Effective Are Antimicrobial Agents on Preventing the Adhesion of Candida Albicans to Denture Base Acrylic Resin Materials? A Systematic Review. *Polymers* **2022**, *14*, 908. [CrossRef]
31. Mohammed, N.B.; Daily, Z.A.; Alsharbaty, M.H.; Abullais, S.S.; Arora, S.; Lafta, H.A.; Jalil, A.T.; Almulla, A.F.; Ramírez-Coronel, A.A.; Aravindhan, S.; et al. Effect of PMMA Sealing Treatment on the Corrosion Behavior of Plasma Electrolytic Oxidized Titanium Dental Implants in Fluoride-Containing Saliva Solution. *Mater. Res. Express* **2022**, *9*, 125401. [CrossRef]
32. Yamada, M.; Fukumoto, M.; Nakano, H.; Isago, H. Cold Spraying of TiO_2 Photocatalyst Coating with Nitrogen Process Gas. *J. Therm. Spray Technol.* **2010**, *19*, 1218–1223. [CrossRef]
33. Darwish, G.; Barão, V.A.; Wu, C.D.; Knoernschild, K.; Huang, S.; Taukodis, C.G.; Bishal, A.K.; Sukotjo, C.; Yang, B.; Campbell, S. Improving Polymethyl Methacrylate Resin Using a Novel Titanium Dioxide Coating. *J. Prosthodont.* **2019**, *28*, 1011–1017. [CrossRef] [PubMed]
34. Nobre, C.M.G.; Hannig, M.; Pütz, N. Adhesion of Hydroxyapatite Nanoparticles to Dental Materials under Oral Conditions. *Scanning* **2020**, *2020*, 6065739. [CrossRef] [PubMed]
35. Carbaugh, D.J.; Parthiban, R.; Rahman, F.; Wright, J.T. Photolithography with Polymethyl Methacrylate (PMMA). *Semicond. Sci. Technol.* **2015**, *31*, 025010. [CrossRef]
36. Li, Z.; Qi, Q.; Sun, J.; Lan, J. Effect of a Denture Base Acrylic Resin Containing Silver Nanoparticles on Candida Albicans Adhesion and Biofilm Formation. *Gerodontology* **2014**, *33*, 209–216. [CrossRef]
37. Sivakumar, I.; Rao, B.; Kamaraj, B.; Sajjan, S.; Arunachalam, K.S.; Ramaraju, A.V. Incorporation of Antimicrobial Macromolecules in Acrylic Denture Base Resins: A Research Composition and Update. *J. Prosthodont.* **2013**, *23*, 284–290. [CrossRef]
38. Kamonwannasit, S.; Phatai, P.; Butburee, T.; Karaphun, A.; Khemthong, P.; Futalan, C.M. Synthesis of Copper-Silver Doped Hydroxyapatite via Ultrasonic Coupled Sol-Gel Techniques: Structural and Antibacterial Studies. *J. Sol-Gel Sci. Technol.* **2020**, *96*, 452–463. [CrossRef]
39. Maleki-Ghaleh, H.; Omidi, Y.; Beygi-Khosrowshahi, Y.; Kavanlouei, M.; Moradpur-Tari, E.; Adibkia, K.; Khademi-Azandehi, P.; Koc, B.; Barar, J.; Kumar, A.P.; et al. Antibacterial and Cellular Behaviors of Novel Zinc-Doped Hydroxyapatite/Graphene Nanocomposite for Bone Tissue Engineering. *Int. J. Mol. Sci.* **2021**, *22*, 9564. [CrossRef]
40. Fatimah, I.; Nugroho, B.H.; Hidayat, H.; Purwiandono, G.; Yahya, A.; Ibrahim, S.; Sagadevan, S.; Citradewi, P.W.; Mohd Ghazali, S.A.I.S. Biosynthesized Gold Nanoparticles-Doped Hydroxyapatite as Antibacterial and Antioxidant Nanocomposite. *Mater. Res. Express* **2021**, *8*, 115003. [CrossRef]